Ancient TL

www.ancienttl.org · ISSN: 2693-0935

Issue 28(2) - December 2010
https://doi.org/10.26034/la.atl.v28.i2

This issue is published under a Creative Commons Attribution 4.0 International (CC BY):
https://creativecommons.org/licenses/by/4.0

© Ancient TL, 2010

Ancient TL

A periodical devoted to Luminescence and ESR dating

Institute of Geography and Earth Sciences, Aberystwyth University,
Ceredigion SY23 3DB, United Kingdom

Volume 28 No.2 December 2010

Estimating the error in equivalent dose values obtained from SAR
G.W. Berger ____ 55

Thesis abstracts
Á. Novothny ____ 67
Q-S. Fan ____ 67
A. Kunz ____ 68
A.Madsen ____ 69

Bibliography ____ 71

Announcements
13th International LED Conference, Toruń, Poland ____ 79
UK Luminescence and ESR Meeting, Aberystwyth ____ 80

Errata: An alternate form of probability-distribution plots for D_e values
G.W. Berger ____ 81

ISSN 0735-1348

Ancient TL

Started by the late David Zimmerman in 1977

EDITOR

G.A.T. Duller, Institute of Geography and Earth Sciences, Aberystwyth University, Ceredigion SY23 3DB, United Kingdom (ggd@aber.ac.uk)

EDITORIAL BOARD

I.K. Bailiff, Luminescence Dosimetry Laboratory, Dawson Building, University of Durham, South Road, Durham DH1 3LE, United Kingdom (ian.bailiff@durham.ac.uk)
S.H. Li, Department of Earth Sciences, The University of Hong Kong, Pokfulam Road, Hong Kong, China (shli@hku.hk)
R.G. Roberts, School of Geosciences, University of Wollongong, Wollongong, NSW 2522, Australia (rgrob@uow.edu.au)
H.P. Schwarcz, School of Geography and Geology, McMaster University, Hamilton, Ontario L8S 4M1, Canada (schwarcz@mcmaster.ca)

REVIEWERS PANEL

R.M. Bailey, Oxford University Centre for the Environment, Dyson Perrins Building, South Parks Road, Oxford OX1 3QY, United Kingdom (richard.bailey@ouce.ox.ac.uk)
G.W. Berger, Quaternary Sciences Center, Desert Research Institute, Reno, Nevada 89506-0220, U.S.A (glenn.berger@dri.edu)
J. Faïn, Laboratoire de Physique Corpusculaire, 63177 Aubière Cedex, France (jean.fain@wanadoo.fr)
R. Grün, Research School of Earth Sciences, Australian National University, Canberra ACT 0200, Australia (rainer.grun@anu.edu.au)
T. Hashimoto, Department of Chemistry, Faculty of Sciences, Niigata University, Niigata 950-21, Japan (thashi@curie.sc.niigata-u.ac.jp)
D.J. Huntley, Department of Physics, Simon Fraser University, Burnaby B.C. V5A1S6, Canada (huntley@sfu.ca)
M. Krbetschek, Saxon Acad. of Sc., Quat. Geochrono. Sect., Inst. Of Appl. Physics / TU Freiberg, Leipziger-Str. 23, D-09596 Freiberg, Germany (quatmi@physik.tu-freiberg.de)
M. Lamothe, Dépt. Sci. de la Terre, Université du Québec à Montréal, CP 8888, H3C 3P8, Montréal, Québec, Canada (lamothe.michel@uqam.ca)
N. Mercier, Lab. Sci. du Climat et de l'Environ, CNRS-CEA, Av. de la Terrasse, 91198, Gif sur Yvette Cedex, France (norbert.mercier@lsce.cnrs-gif.fr)
D. Miallier, Laboratoire de Physique Corpusculaire, 63177 Aubière Cedex, France (miallier@clermont.in2p3.fr)
S.W.S. McKeever, Department of Physics, Oklahoma State University, Stillwater Oklahoma 74078, U.S.A. (stephen.mckeever@okstate.edu)
A.S. Murray, Nordic Laboratory for Luminescence Dating, Risø National Laboratory, Roskilde, DK-4000, Denmark (andrew.murray@risoe.dk)
N. Porat, Geological Survey of Israel, 30 Malkhe Israel St., Jerusalem 95501, Israel (naomi.porat@gsi.gov.il)
J.R. Prescott, Physics Dept., University of Adelaide, Adelaide 5005, South Australia, Australia (john.prescott@adelaide.edu.au)
D. Richter, Department of Human Evolution, Max-Planck-Institute for Evolutionary Anthropology, Leipzig 04103, Germany (drichter@eva.mpg.de)
A.K. Singhvi, Rm 203, Physical Research Laboratory, Navrangpura, Ahmedabad 380009, India (singhvi@prl.res.in)

Ancient TL

A periodical devoted to Luminescence and ESR dating

Web site: http://www.aber.ac.uk/ancient-tl

Institute of Geography and Earth Sciences
Aberystwyth University SY23 3DB
United Kingdom

Tel: (44) 1970 622606 Fax: (44) 1970 622659 E-mail: ggd@aber.ac.uk

Estimating the error in equivalent dose values obtained from SAR

G. W. Berger

Desert Research Institute, 2215 Raggio Parkway, Reno, NV 89512, USA
(e-mail: glenn.berger@dri.edu)

(Received 26 September 2010; Final form 4 December 2010)

Abstract
Central to all aspects of application of SAR (Single-Aliquot-Regenerative-dose) procedures to dating is the accurate estimation of errors in equivalent dose values (D_e). Some approximation approaches have been outlined by others. Here a more rigorous approach is outlined that incorporates the contributions to the total error in D_e from not only error in L_0/T_0 (undosed and unbleached ratio) and the contribution from the scatter of data about the best-fit curve, but also contributions from errors in the best-fit regression parameters and from their covariances. Unequal weighting of data points is included. Algorithms and procedures are detailed for two [saturating exponential (E), and saturating exponential-plus-linear (E+L)] of the 4 most common dose-response models [which include linear (L) and quadratic (Q)]. Computed D_e values and errors are compared for 6 new and three previously published data sets, using the approach of this paper and two of the approaches of Duller (2007). Differences in D_e and its error estimate from these comparisons are often, but not always, small and insignificant, thus indicating that errors in best-fit parameters and their covariances make a small contribution to total error in D_e in most situations. One example data set evaluates the effects of dose-point spacing on the estimated D_e error.

Introduction
As in Duller (2007), Berger (1990, hereinafter "B90") and Berger et al. (1987, hereinafter, "BLK87"), and some other authors (e.g., Grün and Rhodes, 1992), the error analyses presented herein are intended to capture the effects of random errors, not systematic errors. Discussions about the relative role of random and systematic errors in the construction of dose-response curves (DRCs) for TL (thermo-luminescence), ESR (electron spin resonance), and OSL (optically stimulated luminescence) data have been joined by many authors (e.g., BLK87; Grün and Rhodes, 1992; Grün and Packman, 1993; Hayes et al., 1998; Galbraith, 2002). In the case of SAR applications, low signals could lead to dominance of systematic errors whereas larger signals are expected to lead to dominance of random errors in L/T ratios (test-dose-normalized OSL in the SAR approach).

The widely used *Analyst* software package that accompanies the Risø luminescence reader systems provides SAR D_e regression procedures for the L, Q, E and E+L DRC models.

The D_e error estimation procedures of *Analyst* are summarized by Duller (2007). His procedure essentially combines in quadrature two components of the total analytical error in D_e: an interpolated-range (L_0/T_0 ±error) effect, and the effect of scatter (Duller's equation 7) of L/T ratios about the best-fit curve. This interpolated-range procedure is adopted here in the E+L regression model. Duller's (2007) approach does not capture the effects of errors in the fitting parameters, nor any effects of covariances among the errors in these parameters. His approach does, however (Duller, pers. comm., 2010) incorporate the effects of assigning unequal weights to the data points, where weighting is by inverse variance of the estimated absolute errors in L/T ratios.

The importance of weighting in regression and error analysis has been emphasized and discussed elsewhere (e.g., BLK87; B90; Grün and Rhodes, 1992; Grün and Packman, 1993; Hayes et al., 1998) with regard to constructing DRCs for extrapolation to D_e values (in TL and ESR dating). For such extrapolated regressions, Hayes et al. (1998) point out that Bluszcz (1988) discussed how to deal (using the Monte Carlo approach) with TL/ESR cases of mixed error types (e.g., combinations of constant absolute errors, variable absolute errors, constant relative errors). The above cited authors point out (implicitly or explicitly) that dominance by systematic errors implies constant absolute errors, while dominance by random errors can imply constant relative errors. Grün and Rhodes (1992)

conclude that the effects of constant relative errors can be captured by use of weighting by inverse variance, and that this choice leads to smaller errors in estimated D_e values from extrapolated saturating-exponential (hereinafter, 'E fit') TL/ESR DRCs than does the use of equal weighting, which captures the effects of constant absolute errors. This conclusion of Grün and Rhodes (1992) supports the choice of BLK87 for the use of weighting by inverse variance in the calculation of D_e errors from extrapolated DRCs.

While the above efforts concerned extrapolation of DRCs, SAR employs interpolation (as does the regeneration TL procedure). Therefore, estimation of errors in SAR D_e values may have a different dependency on the germane empirical factors than in the case of extrapolations. With SAR, because of the nature of the measurement of L/T ratios, estimation of variance in each SAR dose-data point is quite tractable (e.g., Galbraith, 2002). Thus use of weighting by inverse variance of L/T ratios as presented in this paper is straightforward, avoiding the kinds of uncertainties embedded with the measurement of (for example) TL signals (e.g., BLK87, Appendix A).

Here the mathematical procedures of BLK87 and B90 are adapted to the SAR conditions. BLK87 and B90 used the Gauss-Newton method of linearization of the mathematically non-linear E and E+L models to obtain fitting parameters, and the 'delta' method to obtain error estimates in the extrapolated D_e values. The procedures of BLK87 are statistically accurate when relative errors in the data points are small (e.g., <5%).

Results from these adapted procedures are compared below to the results from the two error-estimation approaches of Duller (2007) as executed in *Analyst* 2007 (v.3.24): his 'curve-fitting' and Monte Carlo approaches. His 'curve-fitting' approach captures the effects mentioned above (error in L_0/T_0, unequal weighting, data scatter about the DRC). His Monte Carlo approach presumably captures the end effects of all empirical variables. As Duller (2007) reminds us, when L_0/T_0 is near the saturation value of E fits, the error in D_e, likely will not be symmetrical. In this situation, only the Monte Carlo approach may yield a statistically accurate estimate of the error in D_e. To construct the best-fit DRCs, Duller (2007) employed the Levenberg-Marquardt (L-M) algorithm. This has many advantages (e.g., Press et al., 1986; Hayes et al., 1998), not the least of which can be speed of convergence for mathematically non-linear models. Essentially then, the algorithms of this paper employ weighting of L/T ratios by inverse variance of same, and, moving beyond the approach of Duller (2007), capture the effects of errors and covariances in fitting parameters.

Although the models presented below force the dose-response curve through the origin, they could be modified to permit passing the regression through the recuperation datum. The 'curve-fitting' procedure of Duller (2007) passes the regression curve through the recuperation datum, but his *Analyst* software permits the choice of forcing the curve through the origin. Since one of the data-acceptance criteria (e.g., Wintle and Murray, 2006) in the use of SAR is the rejection of data for which the recuperation is >1σ or >2σ from zero, forcing the curve through the origin is likely to be usefully accurate in almost all SAR situations. Furthermore, it has been demonstrated empirically (e.g., Ballarini et al., 2007; Berger, 2009; Berger et al., 2010; Cunningham and Wallinga, 2010) that placing the interval selected for 'background' subtraction close to the beginning part of the OSL decay curve, rather than at the end, often has the effect of reducing the recuperation signal to near zero.

Some Nomenclature

The following terms are employed: σ^2 = absolute-error variance; N = number of L/T (hereinafter, "y") data points, including the origin; w = weight, which for SAR is $1/\sigma_y^2$; $y_0 = L_0/T_0$; θ = a fitting parameter (e.g., a, b, or c below); scalar VAR = weighted sum of squares of residuals (an estimate of the scatter of data about the best-fit curve). Note that σ_y^2 can be calculated appropriately by the method of Galbraith (2002). Symmetrical matrix SIG is the matrix Ψ of equation 10 in BLK87 and of equation 4 in B90; and

$$SIG = VAR \cdot (I)^{-1} \qquad (1)$$

That is, SIG is the product of scalar VAR and the inverse matrix of I. Matrix I is the information matrix of BLK87, and thus SIG is the variance-covariance matrix, or error matrix. The diagonal elements of SIG give the variances in the individual fitting parameters, while the off-diagonal elements give the covariances.

Employed throughout this paper is the standard propagation-of-variance equation

$$\sigma^2 = \sum_{k,s} \frac{\partial f}{\partial \theta_k} \frac{\partial f}{\partial \theta_s} \sigma_{\theta_k} \sigma_{\theta_s} \qquad (2)$$

where f is the model function for the curve, and the paired terms provide the variances when k = s and the covariances when k ≠ s. The covariance terms can be

ignored (set to zero) only if the errors in the fitting parameters are independently distributed (independent of each other) and symmetrical with respect to positive and negative values. We assume here that these errors are Gaussian (although this assumption is not required in the approach of BLK87), hence symmetrical, but we cannot assume independence of errors in fitting parameters. However, it is assumed realistically that the error in y_0 is independent of the errors in the fitting parameters. Note that hereinafter, the subscript "i" will be used for summations over the non-zero dose-axis (x) data points.

The elements of the matrix I (when needed below) are derived from equation 11 of BLK87, which reduces to

$$I_{k,s} = \sum_i \frac{1}{f_i^2} \frac{\partial(f_i)}{\partial\theta_k} \cdot \frac{\partial(f_i)}{\partial\theta_s} \qquad (3)$$

Linear Fit

This model, a linear dose response curve passing through the origin, applies to many young sediments or heated materials. Realistically we assume that there are errors in y, not in x. Using the weighted least-squares principle, we wish to minimize

$$S = \sum_i w_i (y_i - f_i)^2 \qquad (4)$$

where f = bx. Deming's (1964) equation 39 (p. 33) provides a straightforward form of S that circumvents the need to know b beforehand, and his equation 34 (p.31) permits easy calculation of slope b.

Inclusion of the effects of scatter of data about the best-fit curve is required. Deming's (1964) equation 41 (p.34) provides a simple formulation of σ_b^2 that includes the data-scatter effect, which he terms the 'external standard error' in b. In our nomenclature, his divisor m-1 in this equation is N-2. Thus, the total variance in D_e is

$$\sigma_{D_E}^2 = D_E^2 \left[\left(\frac{\sigma_b}{b}\right)^2 + \left(\frac{\sigma_{y_0}}{y_0}\right)^2 \right] \qquad (5)$$

Here we assume realistically that there is no covariance of y_0 and b, that is, that the errors in y_0 and b are independent.

Quadratic Fit

This model applies to young sediments for which the dose response curve is supralinear (e.g., Berger, 1987) or to dose response curves that are slightly sublinear. As BLK87 show, in the low dose region of a dose response, a second-order polynomial can be a good approximation to the physically realistic saturating exponential. The Q model is

$$f = bx + cx^2 \qquad (6)$$

and we wish to minimize equation 4 to obtain estimates of b and c.

We use the matrix normal equations, simplified to the case of only one curve (not the intersection of two curves as in BLK87). Then in the case of unequal weights, the coefficients b and c are calculated from equation 2 of BLK87. Following the procedural steps of BLK87, we iterate the calculation of b and c until the difference between successive estimates meets some pre-set convergence limit. The D_e value is the absolute value of the solution to equation 6 when f is replaced by y_0 and x is replaced by D_e.

To obtain the errors in b and c, we need scalar VAR and matrix I from equation 1. Then

$$VAR = \frac{\sum_i w_i (y_i - f_i)^2}{N-3} \qquad (7)$$

with denominator N-3 because there are only two fitting parameters. From equation 3, the elements of matrix I are $I_{bb} = \sum_i w_i x_i^2$, $I_{cc} = \sum_i w_i x_i^4$, $I_{bc} = I_{cb} = \sum_i w_i x_i^3$. Here, the covariances (off-diagonal elements) are not zero because the errors in b and c are not independently distributed. Therefore, using equations 1 and 7, we obtain the elements SIG_{bb}, SIG_{cc} and SIG_{bc} of the error matrix SIG.

The total variance in D_e follows from equation 2 as

$$\sigma_{D_E}^2 = \left(\frac{\partial f}{\partial y_o}\right)^2 \sigma_{y_0}^2 + \left(\frac{\partial f}{\partial b}\right)^2 SIG_{bb} + \left(\frac{\partial f}{\partial c}\right)^2 SIG_{cc} + 2\left[\frac{\partial f}{\partial b} \cdot \frac{\partial f}{\partial c} \cdot SIG_{bc}\right] \qquad (8)$$

where we assume reasonably that the error in y_0 is independent of the errors in b and c. Therefore, applying equation 8 to the analytic formula for D_e (solution to equation 6), equation 8 becomes

$$\sigma_{D_E}^2 = \left(\frac{\sigma_{y_0}}{Z}\right)^2 + \left(\frac{b}{2c(Z-1)}\right)^2 SIG_{bb} + \left(\frac{y_0 - ZD_E}{cZ}\right)^2 SIG_{cc} + 2\left[\left(\frac{b}{2c(Z-1)}\right)\left(\frac{y_0 - ZD_E}{cZ}\right) SIG_{bc}\right] \qquad (9)$$

where $Z = |b^2 - 4c(-y_0)|$.

Saturating Exponential (E)
This model has the most general applicability to charge-trap physical processes, for which trap-type filling at high doses can occur. The model is

$$f = a(1-e^{-bx}) \quad (10)$$

and we wish to minimize equation 4 to obtain estimates of parameters a and b. From equation 10,

$$D_e = \frac{1}{b} ln \left[\frac{a}{a-y_0}\right] \quad (11)$$

since $f = y_0$ when $x = D_e$.

Regression to obtain a and b
We use the matrix methods and follow the steps of BLK87. The suggested procedure of BLK87 begins with obtaining initial (trial) estimates of a and b by setting the weight matrix = 1 and using a quadratic form of the dose-response curve. This step gives initial estimates of a and b.

Then using estimated (calculated) weights, we find increments to a and b using equation 9 of BLK87. In practice, equation 9 can be reformulated (BLK87 matrix symbol β replaced here by matrix symbol ΔA) to:

$$\Delta A = ([WU]^t[WU])^{-1}([WU]^t[WY^*]) \quad (12)$$

where the matrix elements are:
$wu_a = (1 - e^{-bx_i})\sqrt{w_i}$,
$wu_b = ax_i e^{-bx_i}\sqrt{w_i}$,
$wy^* = y_i - a(1 - e^{-bx_i})\sqrt{w_i}$.

Equation 12 is iterated to the desired level of convergence of a and b. Then D_e is calculated from equation 11.

Error in D_e
We use equation 2, with the D_e from equation 11 replacing f in equation 2. Thus the variance in D_e is calculated from equation 8 (with b, c replaced by a, b respectively). Using equation 10, we obtain the elements of I:
$I_{aa} = \sum_i w_i$,
$I_{bb} = \sum_i w_i (x_i e^{-bx_i})^2$,
$I_{ab} = I_{ba} = \sum_i w_i f_i e^{-bx_i}$

Elements of SIG are obtained from equation 1. Using equation 11 for D_e, the partial derivatives in equation 8 become:

$$\frac{\partial D_E}{\partial y_0} = [b(a - y_0]^{-1},$$
$$\frac{\partial D_E}{\partial a} = -y_0/ab(a - y_0) \text{ and}$$
$$\frac{\partial D_E}{\partial b} = -D_E/b .$$

These results then permit the calculation of the variance in D_e.

Saturating Exponential Plus Linear (E+L)
This model, as stated by B90, is physically realistic when charge-trap creation occurs at high doses. The linear term can represent the trap-type creation region of the dose response curve. Dose response curves with apparent linear growth superimposed upon a saturating exponential growth have been observed under laboratory irradiations in TL dating (e.g., B90) and quartz SAR OSL dating (e.g., Murray et al., 2008; Pawley et al., 2008). Does this E+L laboratory response of test-dose-normalized OSL require the assumption of E+L trap filling under natural irradiation (sediment burial) conditions? Notwithstanding this question, comparison of quartz SAR OSL age estimates derived from use of an E+L dose response curve model with independent ages have shown good agreement at ~ 200 ka (Seyda River sites, Murray et al., 2008) and at ~ 450 ka (Pawley et al., 2008). On the other hand, Lai (2010) reported dramatic age under-estimation for old loess when E+L dose response curves were observed. Could this under-estimation be partly an effect of differences in his SAR procedure from those of others (e.g., Murray and Wintle, 2003)?

There is another physically realistic model that can mimic an apparent E+L dose response curve in SAR, and this is the 'double-saturating-exponential' (DSE) model (e.g., Wintle and Murray, 2006). Here the apparent linear term can manifest a second set of charge traps with a different (larger) saturation level than the first type. Murray et al. (2007) employed this model with SAR data for quartz from their Sula River sites, but obtained age underestimates. Murray et al. (2008) discussed this result, and suggested that perhaps the nature of the geological setting at Sula River and of the independent age assignments might have had more influence on this underestimate than any putative instability in the quartz SAR signal from the high-dose region of the dose response curve. However, in this report only the E+L model is considered for error analysis because this model is much more tractable than the DSE model.
The model is

$$f = a(1-e^{-bx}) + cx \quad (13)$$

A straightforward, efficient and acceptably accurate path to follow is to use equation 13 to obtain a, b, c, VAR and SIG, then to use

$$f' = y_0 - a(1-e^{-bx}) - cx \qquad (14)$$

to solve for D_e, because $f' = 0$ when $x = D_e$. Equation 14 can be solved for D_e very efficiently by using the Newton-Raphson iterative procedure (e.g., McCalla, 1967).

Regression to obtain a, b, c

As for the E case, we use the quadratic model with weights = 1 to obtain initial estimates of a and b. Then we assign an initial estimate for c of (e.g.) 0.005, based on the likely general increase in L/T as a fraction of applied dose in units of sec. With these initial estimates of a, b and c, we use equation 12 to begin the iterative process to refine these estimates toward some limit of convergence. In this case, the elements of matrices WU and WY* become:

$wu_a = (1 - e^{-bx_i})\sqrt{w_i}$,
$wu_b = (ax_i e^{-bx_i})\sqrt{w_i}$,
$wu_c = x_i\sqrt{w_i}$, and
$wy^* = [y_i - a(1 - e^{-bx_i}) - cx_i]\sqrt{w_i}$.

Solution for D_e and error in D_e

Once we have a, b and c, we can use equations 14 to iteratively solve for D_e. Here, the estimation of errors in D_e is more complex than for the previous models. An efficient, fast and reasonably accurate procedure is to approximate the total variance in D_e as

$$\sigma^2_{D_E} = \sigma^2_{D_E}(y_0) + \sigma^2_{D_E}(\theta) \qquad (15)$$

which is the sum of variances from the effect on D_e of error in y_0 and the variance arising from the combination of the effects of data scatter about the best-fit curve with the variances and covariances in the fitting parameters a, b and c.

Error in D_e arising from error in y_0

An historically effective way (and used by Duller, 2007) to estimate the component of variance in D_e that relates to the effects of the variance in y_0 is to iterate the solution of equation 14 under 3 conditions:

(i) set $y_0' = y_0 + \sigma_{y_0}$, obtain D_e' ;
(ii) set $y_0'' = y_0 - \sigma_{y_0}$, obtain D_e'' ;
and (iii) set $y_0' = y_0$, obtain the best-fit D_e.

Although $\sigma^2_{D_E}(y_0)$ may not always be symmetrical about D_e, it is acceptable to set

$$\sigma^2_{D_E}(y_0) = [(D_E' - D_E'')/2]^2 \qquad (16)$$

Error in D_e arising from data scatter and from errors in a, b and c

For this purpose we can use the efficient equation 4 of B90 (with his Ψ replaced by our SIG), which captures all the effects we wish to incorporate. Then in that equation 4,

$V^t = \left(\frac{\partial f}{\partial a}, \frac{\partial f}{\partial b}, \frac{\partial f}{\partial c}\right)$
$= ([1 - e^{-bx}],\ axe^{-bx},\ x)$, and
$\frac{\partial f}{\partial D_E} = c + abe^{-bD_E}$.

For use in equation 1 we need

$VAR = \sum_i \frac{w_i(y_i - f_i)^2}{N-4}$

where f_i is given by equation 13. The elements of I, derived using equation 3, are:

$I_{aa} = \sum_i w_i(1 - e^{-bx_i})^2$,
$I_{bb} = \sum_i w_i(ax_i e^{-bx_i})^2$,
$I_{cc} = \sum_i w_i {x_i}^2$,
$I_{ab} = I_{ba} = \sum_i w_i a x_i e^{-bx_i}(1 - e^{-bx_i})$,
$I_{ac} = I_{ca} = \sum_i w_i x_i(1 - e^{-bx_i})$,
$I_{bc} = I_{cb} = \sum_i w_i a x_i^2 e^{-bx_i}$.

Therefore, with these equations for the elements of matrix I and the equation for VAR, we obtain $\sigma^2_{D_E}(\theta)$ from equation 4 of B90 and the total variance in D_e from equation 15 combined with equation 16.

Comparison of Results from Data Sets

Results from 3 error-estimation approaches are compared below. The first two approaches are the 'curve-fitting' and Monte Carlo routines of Duller (2007) outlined in the first section and executed in *Analyst* 2007, and the third is the approach outlined in this paper.

Duller's data sets

Table 1 lists comparisons of the D_e and errors for 3 of Duller's (2007) multi-grain SAR data sets. Duller's (2007) data set D-4 illustrates a linear (L) regression, and the other two, a saturating exponential (E) (samples D-1 and D-2). The E data sets of Duller (2007) are only somewhat sublinear. There is no significant difference in error estimates (within 1σ)

Sample	Model	Equivalent Dose (Gy)		
		Curve Fitting	Monte Carlo[a]	This paper
D-4	L	0.71 ± 0.11	± 0.13(Sym)	0.73 ± 0.11
D-1	E	0.70 ± 0.06	± 0.06(Sym)	0.698 ± 0.058
D-2	E	28.50 ± 0.67	± 0.75(Sym)	28.48 ± 0.68

[a] 1000 repeats were used. 'Sym' means that the D_e distribution is symmetric. Only the uncertainties are reported because the D_e estimates are those from the curve-fitting scheme

Table 1: *Comparison of equivalent dose values, and 1σ uncertainties, for 3 data sets from Duller (2007).*

Sample	FUS-1 (1-70) [a]	FUS-1 (2-20)	FUS-1 (4-40)		SFC-6 (A-10)	SFC-6 (A-15)		ATP-37 (A-1)
Dose (s)	*L/T*	*L/T*	*L/T*	*Dose (s)*	*L/T*	*L/T*	*Dose (s)*	*L/T*
Natural	1.390 ± 0.378	1.261 ± 0.383	1.703 ± 0.538	Natural	4.957 ± 0.208	2.671 ± 0.212	Natural	4.500 ± 0.107
100	0.091 ± 0.110	0.324 ± 0.139	0.200 ± 0.234	100	1.109 ± 0.053	1.146 ± 0.107	150	0.814 ± 0.021
300	0.352 ± 0.127	0.900 ± 0.455	0.750 ± 0.322	250	2.129 ± 0.092	2.023 ± 0.195	300	1.379 ± 0.034
1000	1.452 ± 0.483	1.909 ± 0.796	1.783 ± 0.649	500	3.278 ± 0.137	2.165 ± 0.178	700	2.360 ± 0.057
0	-0.036 ± 0.037	-0.074 ± 0.057	0.001 ± 0.001	1000	4.306 ± 0.172	3.420 ± 0.288	1200	3.209 ± 0.077
Recycle	1.0 ± 1.6	1.01 ± 0.58	2.4 ± 3.0	2000	5.592 ± 0.226	3.390 ± 0.269	2000	3.925 ± 0.094
				0	-0.023 ± 0.012	-0.022 ± 0.024	2800	4.558 ± 0.108
				Recycle	0.87 ± 0.06	1.07 ± 0.14	3600	4.853 ± 0.114
							4200	5.091 ± 0.120
							5000	5.441 ± 0.128
							5800	5.737 ± 0.135
							7000	6.102 ± 0.143
							0	0.005 ± 0.002
							Recycle	0.88 ± 0.03

[a] In parenthesis, either the 'single'-grain hole (e.g., disc 1, hole 70) or the multi-grain aliquot number. The recycle ratio is for the first applied dose. The FUS and SFC samples are quartz sand grains (respectively, 125-185 μm and 105-212 μm). The ATP-37 sample is 4-11 μm quartz.

Note: Most L/T errors in this table are listed with a precision of 3 significant digits even though it is well known that most data error estimates themselves have uncertainties typically of 10-30% (e.g., Topping, 1962, p. 89-90). The retention of 3 significant digits is intended to minimize any effects of round-off error for those users who wish to employ these data in comparisons of results from their own models with the models in this paper. These L/T ratios are from the screen display of Analyst, which truncates errors to the third decimal place. Note also that the absolute errors in the ATP-37 L/T ratios yield approximately constant relative errors (~2.5%).

Table 2: *Example data for regression models*

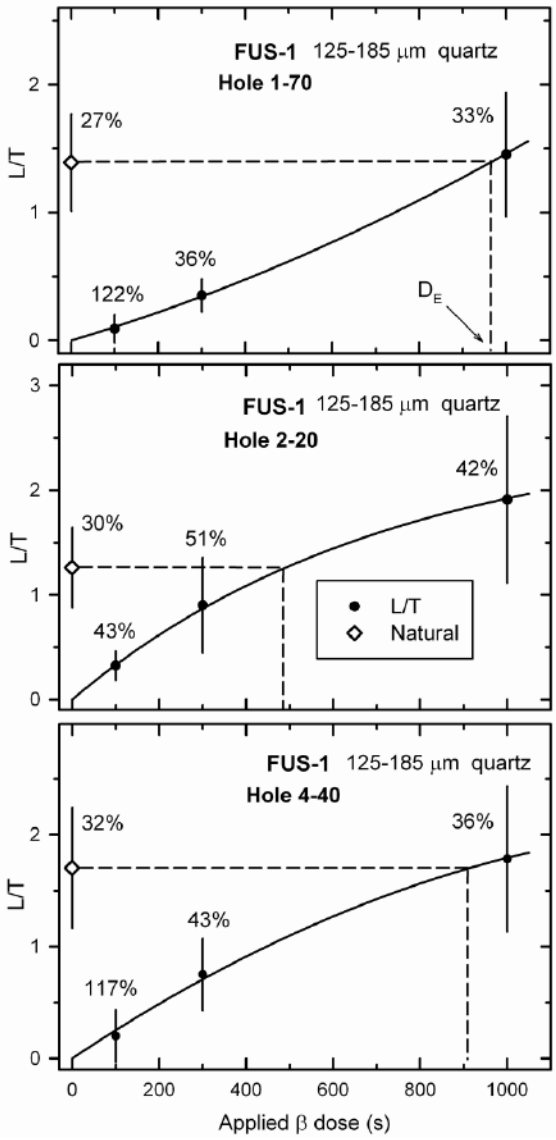

Figure 1: *Top to bottom, Q, E and Q regressions using the routines of this paper for the 'single-grain' FUS-1 data in Table 2. The percent relative error in each L/T ratio is shown.*

among the 3 approaches for the samples D-4, D-1, and D-2. For these data, the fitting parameters (not shown) generated by *Analyst* 2007 and by the author's routines do not differ by more than a small fraction of the 1σ uncertainties in these parameters. That is, the respective best-fit DRCs do not differ noticeably.

Author's data sets

The 6 data sets of the author listed in Table 2 illustrate the use of the Q, E and E+L models. Unlike in Duller's (2007) examples, the dose points in Table 2 are in seconds, not Gy. Other distinctions are in the footnotes to Table 2. The data for the first 3 examples

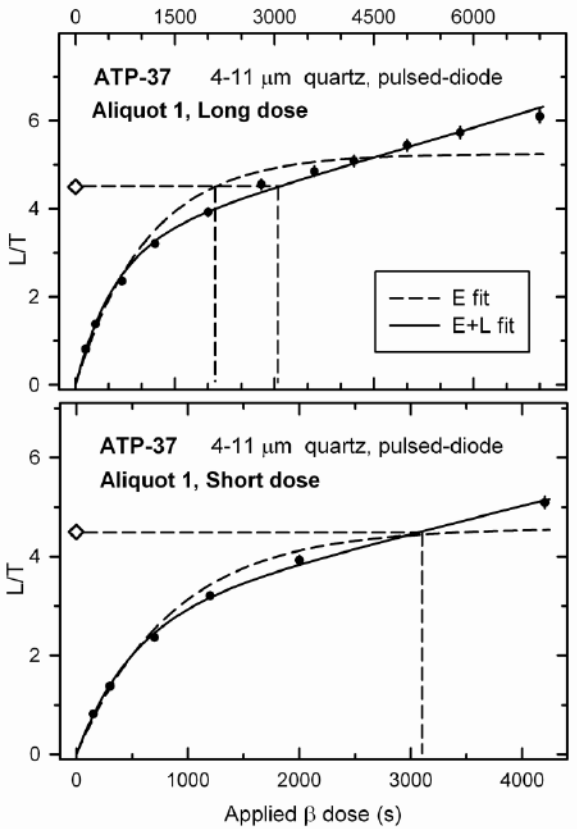

Figure 2: *Comparison of E and E+L best-fit DRCs for sample ATP-37.*

represent SAR conditions for which the relative errors in the L/T ratios are much larger than those in the data sets of Duller (2007). These larger errors manifest the effects of low signals, and so it is likely that the role of systematic errors is larger than would otherwise be the case. Furthermore, these 3 data sets were selected because the scatter of the data about the best-fit DRCs is very small while the absolute and relative errors in the L/T ratios are very large. Finally, the corresponding fitting parameters have very large relative errors (as estimated by *Analyst* 2007).

The data (excluding recycle and recuperation points) for the 3 different grains of the FUS-1 sample are plotted in Fig. 1, with best-fit regressions of the Q (top), E (middle), and Q (bottom) models. The best-fit DRCs of *Analyst* 2007 and of the author do not differ on the scale of these plots. All data have large relative errors. The relative errors in the L_0/T_0 ratios are comparable in all 3 plots. The relative errors in the dose response curve data in the top and bottom plots are comparable, but differ from those in the middle plot. Examples of single-grain data having similarly large relative errors but with more variability within the dose response curve could

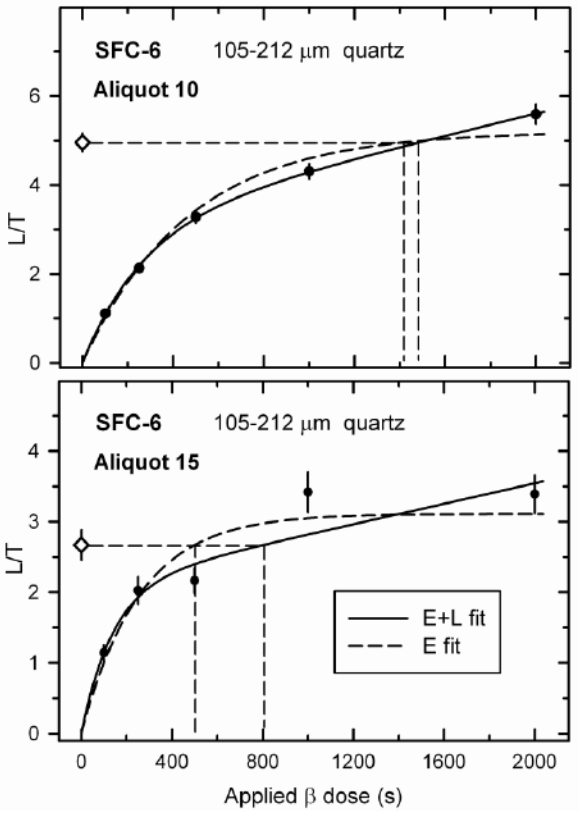

Figure 3: *Comparison of E and E+L best-fit DRCs for sample SFC-6.*

probably be found by the author and by readers, but these examples are sufficient to illustrate some differences in the results from the different error-analyses schemes. The D_e and error results from FUS-1 are discussed below after presenting plots for the remaining data in Table 2.

The multi-grain SAR data for the fine-silt (4-11 μm) quartz of sample ATP-37 are presented not only because they provide DRCs having a nearly 'linear' portion beyond a saturating exponential, but also to illustrate the effects on estimated errors in D_e values of variations in the spacing of dose points. The dose points for the ATP-37 data are approximately equally spaced beyond 1000 s. For extrapolated D_e estimation, the simulations of Grün and Rhodes (1992) showed that doubling of the dose-point spacing (as usually practiced by the author and by BLK87 and B90 for non-SAR data) was preferred to equal spacing of dose points because dose doubling led to smaller errors in the D_e values. However, it is not clear what the effects of different dose-point spacings might be on D_e values and errors calculated for SAR dose response curves (which employ interpolation for D_e estimation). From these ATP-37 data, the dose-doubling scenario can be approximated by eliminating certain dose points in the regressions.

The ATP-37 data for the complete dose range are plotted in the top of Fig. 2, with both E and E+L regressions illustrated. As for the FUS-1 data, the best-fit response curves of the author and of *Analyst* 2007 are indistinguishable at the plotting scale (the fitting parameters agree within their first 3 digits). The bottom of Fig. 2 shows regressions for an approximate 'dose-doubling' scenario, over a truncated dose range (to 4.2 ks, rather than 7 ks).

It is immediately clear in the top of Fig. 2 that the choice of regression model has a dramatic effect on the value of the estimated D_e and that the weighted E model is inappropriate. An equal-weighting (unweighted) E model has not been applied to these data, but it is not expected to provide an acceptable fit. In the lower Fig. 2, a D_e value could not be computed by either *Analyst* 2007's or the author's weighted E-fit routines, because the E fit saturates near the L_0/T_0 value. So in this example incomplete knowledge of the DRC could lead to rejection of the aliquot if only an E model were applied.

The final example data set in Table 2 (sample SFC-6) is a dose-doubling set from a multi-grain dating experiment of the author. The best-fit dose response curves are plotted in Fig. 3. Aliquot 10 (top) represents the form of the dose response for most of the 21 aliquots of this sample: apparently an E+L fit is most appropriate. *Analyst* 2007 provides a 'fit' (estimate of weighted sums of squares of residuals about the best-fit dose response) value of 0.0132 for the E+L model and 0.0959 (~ 7 times larger) for the E model. However, as is shown below, the 3 error-estimation schemes report no statistical difference (at 1σ) in the D_e values from these weighted E and E+L fits.

Aliquot 15 (bottom, Fig. 3) was selected because not only do the data scatter more widely about the best-fit weighted regression dose response, but also the errors in the L/T ratios are much larger than for aliquot 10. In this case, to a first approximation, it could be acceptable to prefer the E+L model based on the assumption that all quartz in this sample should behave the same way. Generally, however, experience shows that quartz dose response curves can vary from grain to grain within a given sample. Therefore, if there are few grains per aliquot, one could expect inter-aliquot differences in dose response.

Sample [a]	Model [b]	Equivalent Dose (s)		
		Curve Fitting	Monte Carlo [c]	This paper
FUS-1/1-70	Q	964±202	±429(Sym)	963±204
FUS-1/2-20	E	491±219	±295(+Asym)	491±213
FUS-1/4-40	Q	914±188	±447(-Asym)	914±493
ATP-37/A-1	E(long)	2104±219	±170(Sym)	2104±128
	E+L(long)	3057±227	±262(Sym)	3056±262
	E(short)	sat'n	-	sat'n
	E+L(short)	3095±185	±224(Sym)	3092±251
SFC-6/A-10	E	1417±769	±171(Sym) [d]	1417±148
	E+L	1489±162	±213(Sym)	1487±172
SFC-6/A-15	E	502±160	±99(Sym)	-- [e]
	E+L	807±299	±314(+Aysm)	806±441

Notes:
a: 'n-m' indicates 'single-grain' disc-hole number; 'A-n' indicates aliquot number.
b: For ATP-37, 'long' means 0-7 ks dose range, while 'short' means 0-4.2 ks.
c: 'Sym' indicates a symmetrical distribution in D_e values, whereas '+Asym' denotes asymmetry (high-side skewness) and '-Asym' denotes low-side skewness. For multi-grain aliquots, 700 repeats are used, whereas 1000 repeats are used for single-hole data. *Analyst* 2007 provides a ±1σ error from the Monte Carlo D_e distribution probably by fitting a Gaussian that is centered on the peak of the distribution's histogram. For an asymmetric distribution, this ±1σ error can be misleading. Only error estimates are reported (see footnote 'a', Table 1)
d: Although symmetrical, the corresponding Monte Carlo distribution peak occurs at ~1200±~150(1σ) s, not 1417, and moreover, only 58% of the repeats are fitted (~55% when 1000 repeats are selected).
e: Does not calculate.

Table 3: *Comparison of D_e ± 1σ results for the data in Table 2.*

The *Analyst* 2007 'fit' values (0.118 for the E model, 0.112 for the E+L model) are probably effectively the same for aliquot 15. Thus even though it might appear in lower Fig. 3 that the E and E+L models provide distinctly different D_e values, the results in Table 3 below indicate that they do not differ at 1σ. Thus aliquot 15 is a good example of an ambiguous dose response curve that could provide misleading D_e values for a sediment sample containing mixed-age quartz grains. In light of the lessons from the plots in Fig. 2, SFC-6 provides an example of a sample for which a greater number of dose points should have been chosen, not necessarily evenly spaced.

Comparison of D_e and errors for the Table 2 data sets

The D_e and $\sigma^2_{D_E}$ values obtained from the regressions shown in Figs. 1, 2 and 3 are listed in Table 3, along with corresponding values from Duller's (2007) 'curve fitting' and Monte Carlo procedures.

The Q-fit error estimates for FUS-1(1-70) from Duller's 'curve-fitting' approach and the author's approach are indistinguishable. Although the relative errors in fitting parameters b and c estimated by *Analyst* 2007 are respectively ~50% and ~200%, this agreement between the two approaches implies that the contributions to the total error in D_e from errors in fitting parameters are negligible in this case. However, both D_e errors under-estimate the Monte Carlo error estimate by a factor of about two. Thus for such data (large relative errors, few dose points, little scatter about the best-fit DRC), one should always check the Monte Carlo result before accepting the error estimates from either of the other two approaches.

With the E-fit DRC of FUS-1(2-20), the two smaller error estimates in D_e do not differ significantly and either of the estimates would imply that this 'grain' should be accepted (error estimates in D_e are <50%). The estimated relative errors in fitting parameters a

and b are ~100%. Thus the agreement of the D_e error (±219 s) from the 'curve-fitting' scheme with that (±213 s) from the author's scheme implies that the effect of errors in the fitting parameters on the total D_e error is negligible in this case also. Nevertheless, a visual inspection of the Monte Carlo D_e distribution suggests that a more accurate error estimate would be 491^{+400}_{-300} s (1σ), and therefore that this 'grain' should be rejected. Caveat emptor!

The error estimates for the Q-fit FUS-1(4-40) also are instructive as to relative performance of the different error-estimation schemes. While the *Analyst* 2007 Q-fit estimate of ±188 s would imply that this D_e value should be accepted, the author's scheme produces a much larger estimate (±493 s), suggesting that a closer look at the data is required. Here the estimated relative errors in the fitting parameters b and c are respectively ~50% and ~200%, similar to those for example FUS-1(1-70). Notwithstanding, the author's error estimate is much closer to the Monte Carlo symmetric estimate (±447 s) from Analyst2007, but even this fact is misleading because the Monte Carlo D_e histogram is highly asymmetric and dramatically skewed to smaller values (negative skewness). A visual inspection of this histogram suggests a more appropriate result of 914^{+150}_{-350} s (1σ). Thus in this example, the Duller 'curve-fitting' error-estimation scheme under-performs, and the other two symmetric-error results (Monte Carlo and author's) schemes over-estimate the asymmetric, most-likely error estimates (+150, -350 s).

The ATP-37 data set also offers some useful insights into relative performance of the 3 error-estimation schemes. The full-range ("long") dose E fits give identical D_e values (2104 s) but apparently different error estimates. From the graph (top Fig. 2) it is apparent that the weighted E fits are not appropriate, and from Table 3 it is clear that the D_e values from the E+L model are significantly larger than the E-fit values (by ~50%). What is unexpected is the relatively small E-fit error estimate (±128 s) produced by the author's scheme. The Monte Carlo error estimate is near the middle of the range of errors produced by the schemes of the author and of *Analyst* 2007. These inter-scheme differences for the E model may reflect effects from the use of weighting, but that is a subtlety requiring more study (as suggested by the reviewer, perhaps using numerical simulations, e.g., Grün and Rhodes, 1992). Notwithstanding, the E+L model yields essentially identical results from the 3 approaches, with Analyst2007 giving a 15% (statistically perhaps insignificant) under-estimation of the error (compared to the Monte Carlo result). Is this apparent under-estimation a consequence of not capturing the contributions from the errors and covariances in the fitting parameters? Perhaps only model simulations could answer this question.

Concerning the short-dose regressions, because the L_0/T_0 ratio is at or near the saturation value of the exponential fit, neither *Analyst* 2007 nor the author's scheme could calculate a D_e value from the E model. On the other hand, both schemes produced effectively identical D_e values from the use of the E+L model. Where they differ in this case is that again *Analyst* 2007's 'curve-fitting' scheme yields the lowest error estimate. Again, this may reflect the neglect of the contributions from the errors and covariances in the fitting parameters. What is also helpful to notice is that any effect of changes in the dose-point spacing (compare top and bottom of Fig. 2) on E+L results when the L_0/T_0 intersection is well within the 'linear' part of the dose response is not statistically resolvable with this data set. This suggests that with SAR, the type of dose-point spacing may not be a significant variable in the estimation of D_e and its error, as long as the scatter about the best-fit E+L DRC is small.

The final data set (SFC-6) provides an example of dose responses for which a critical variable may be the number of dose points, not the spacing of same. Aliquot 10 of sample SFC-6 apparently yields essentially identical D_e values whether the E or E+L models are used. However, the error estimates from the use of the E model differ among the 3 schemes, and the *Analyst* 2007 E-fit Monte Carlo D_e histogram is anomalous (footnote 'd'). This Monte Carlo routine did not execute to completion (footnote 'd') so the asymmetric D_e histogram (peak at ~ 1200 s) provides no helpful information about what the statistically realistic D_e error should be. One could certainly expect an asymmetric Monte Carlo D_e distribution from this E-fit example, but a symmetric result is generated. The *Analyst* 2007 'curve-fitting' error estimate of ±769 s for this E fit would appear (from Fig. 3) to be a more reasonable error estimate than those from the other two approaches. For aliquot 10, only the weighted E+L model yields general consistency among the 3 error-analysis schemes, and thus this model is preferred for this aliquot.

As mentioned above, aliquot 15 was selected to represent a dose response having both a larger scatter of L/T ratios about the DRC and larger relative errors (about double) in the L/T ratios than those for aliquot 10. Given the nearness of the L_0/T_0 ratio to the E-fit saturation and the paucity of the dose points, it is surprising how small the error estimates are from the *Analyst* 2007 'curve-fitting' and Monte Carlo

schemes. Neither seems realistic. On the other hand, all 3 schemes yield E+L model error estimates that overlap at 1σ with the E-fit D_e estimates.

Notwithstanding, there are differences among the E+L error estimates, with the *Analyst* 2007 'curve-fitting' providing the smallest estimate and the author's scheme, the largest. This largest estimate (±441) appears to reflect more accurately the large spread (at 2σ) of D_e values within the Monte Carlo histogram than does the 'curve-fitting' error estimate of *Analyst* 2007. However, only the Monte Carlo histogram for the E+L results from aliquot 15 appears to produce a realistic estimate in this case. In particular, this histogram suggests a D_e value of 807^{+300}_{-200} s (1σ). Aliquot 15 yields somewhat ambiguous model results, and without obtaining additional dose points, it is acceptable (to a first approximation) to prefer the E+L model because that seems to be applicable to most of the other aliquots (not shown) from this sample. It is clear that the author's error-analysis scheme could lead to the rejection (D_e error >50%) of this aliquot, whereas the other schemes would not.

Conclusions

Duller's (2007) 'curve-fitting' approach to estimation of errors in SAR D_e values, executed in *Analyst* 2007 software, does not capture the contributions from errors in the regression parameters nor from any covariances among the errors in these parameters. The author's error-analysis schemes do capture these contributions. However, comparisons of the computed D_e values and their error estimates from these two schemes applied to selected data sets generally show no statistically significant differences in error estimates except in special cases.

Moreover, the Monte Carlo scheme executed in *Analyst* 2007 can in some cases indicate a D_e histogram peak at a value significantly different from the 'central D_e value' reported by *Analyst* 2007.

Generally, however, for SAR data that have relatively small scatter about the best-fit dose-response curves and that have relative errors in L/T ratios smaller than ~5%, there are no significant differences among the 3 discussed schemes for analysis of L, Q, E and E+L models.

Nevertheless, some data sets (some presented here) can generate misleading D_e and error estimates, and the practitioner of SAR dating should inspect such data sets carefully before accepting D_e and error estimates, no matter which error-analysis scheme is employed.

Finally, one selected data set (ATP-37, Table 2) provides a good example of quartz SAR E+L dose response, and is used here to demonstrate that there is (in this case) little or no dependence of computed D_e values and their error estimates on dose-point spacing schemes, whether spaced evenly or by dose-doubling. This contrasts with the dose-point-spacing dependency shown by the simulations of Grün and Rhodes (1992) for non-SAR data (for which extrapolation is used).

Acknowledgements

Constructive review comments on the first two drafts of this manuscript by Dr. Kristina Thomsen are greatly appreciated.

References

Ballarini, M., Wallinga, J., Wintle, A.G., Bos, A.J.J. (2007) Analysis of equivalent-dose distributions for single grains of quartz from modern deposits. *Quaternary Geochronology* **2**, 77-82.

Berger, G.W. (1987) Thermoluminescence dating of the Pleistocene Old Crow tephra and adjacent loess, near Fairbanks, Alaska. *Canadian Journal of Earth Sciences* **24**, 1975-1984.

Berger, G.W. (1990) Regression and error analysis for a saturating-exponential-plus-linear model. *Ancient TL* **8**, 23-25.

Berger, G.W. (2009) Zeroing Tests of Luminescence sediment dating in the Arctic Ocean: Review and new results from Alaska-margin core tops and central-ocean dirty sea ice. *Global and Planetary Change* **68**, 48-57.

Berger, G.W., Lockhart, R.A., Kuo, J. (1987) Regression and error analysis applied to the dose response curves in thermoluminescence dating. *Nuclear Tracks and Radiation Measurements* **13**, 177-184.

Berger, G.W., Sawyer, T.L., Unruh, J.R. (2010) Single- and multigrain luminescence dating of sediments related to the Greenville fault, eastern San Francisco Bay area, California. *Bulletin of the Seismological Society of America* **100**, 1051-1072.

Bluszcz, A. (1988) The Monte Carlo experiment with the least squares methods of line fitting. *Nuclear tracks and Radiation Measurements* **14**, 355-360.

Cunningham, A. C., Wallinga, J. (2010) Selection of integration time intervals for quartz OSL decay curves. *Quaternary Geochronology* **5**, 657-666.

Deming, W.E. (1964) *Statistical Adjustment of Data*. Dover Publications, Inc., New York, 255pp.

Duller, G.A.T. (2007) Assessing the error on equivalent dose estimates derived from single aliquot regenerative dose measurements. *Ancient TL* **25**, 15-24.

Galbraith, R. F. (2002) A note on the variance of a background-corrected OSL count. *Ancient TL* **20**, 49-51.

Grün, R., Rhodes, E.J. (1992) Simulation of saturating exponential ESR/TL dose response curves -- weighting of intensity values by inverse variance. *Ancient TL* **10**, 50-56.

Grün, R., Packman, S. (1993) Uncertainties involved in the measurement of TL intensities. *Ancient TL* **11**, 14-20.

Hayes, R. B., Haskell, E. H., Kenner, G. H. (1998) An assessment of the Levenberg-Marquardt fitting algorithm on saturating exponential data sets. *Ancient TL* **16**, 57-62.

Lai, Z. P. (2010) Chronology and the upper dating limit for loess samples from Luochuan section in the Chinese Loess Plateau using quartz SAR protocol. *Journal of Asian Earth Sciences* **37**, 176-185.

McCalla, T.R. (1967) *Introduction to Numerical methods and FORTRAN Programming*. John Wiley & Sons, New York, 351pp.

Murray, A. S., Wintle, A. G. (2003) Luminescence dating of quartz using an improved single-aliquot regenerative-dose protocol. *Radiation Measurements* **37**, 377-381.

Murray, A. S., Svendsen, J. I., Mangerud, J., Astakhov, V. I. (2007) Testing the accuracy of quartz OSL dating using a known-age Eemian site on the river Sula, northern Russia. *Quaternary Geochronology* **2**, 102-109.

Murray, A. S., Buylaert, J-P., Henriksen, M., Svendsen, J-I., Mangerud, J. (2008) Testing the reliability of quartz OSL ages beyond the Eemian. *Radiation Measurements* **43**, 776-780.

Pawley, S. M., Bailey, R. M., Rose, J., Moorlock, B. S. P., Hamblin, R. J. O., Booth, S. J., Lee, J. R. (2008) Age limits on Middle Pleistocene glacial sediments from OSL dating, north Norfolk, UK. *Quaternary Science Reviews* **27**, 1363-1377.

Press, W. H., Flannery, B. P., Teukolsky, S. A., Vetterling, W. T. (1986). *Numerical Recipes: The Art of Scientific Computing*. Cambridge University Press.

Topping, J. (1962) *Errors of Observation and their Treatment*. Chapman and Hall, London, 116pp.

Wintle, A. G., Murray, A. S. (2006) A review of quartz optically stimulated luminescence characteristics and their relevance in single-aliquot regeneration dating protocols. *Radiation Measurements* **41**, 369-391.

Reviewer
K. Thomsen

Thesis Abstracts

Author: Ágnes Novothny
Thesis Title: Luminescence dating of Quaternary aeolian sediments from Hungary
Grade: Ph.D.
Date: December 2008
Supervisor: Manfred Frechen, Erzsébet Horváth
Address: Department of Earth Sciences, Freie Universität Berlin, Germany

Loess, loess-like sediments and aeolian sand cover great areas of Hungary. The study areas of this thesis are located in the Gödöllő Hills and along the right bank of the Danube in North-Hungary, both areas are covered by young aeolian sediments.

Different luminescence methods and techniques were applied in order to find the most appropriate protocol to date the sediments of these regions. First IRSL multiple aliquot methods were used for feldspar and polymineral fine grain samples at Albertirsa, Süttő and Tura. The results were in agreement with the previous dating results from Hungary during the 1990s, mostly measured with the same protocol. However, significant age underestimation was observed in all cases, possibly due to anomalous fading of the feldspars. In the next step single aliquot regeneration protocols were applied for quartz and feldspar. The uncorrected IRSL SAR results basically yielded the same results like those of the IRSL MAAD protocol. However, more precise results were obtained by the SAR protocol, especially for very young samples. The main advantage of the SAR protocol over the MAAD method for the samples investigated in this thesis, that fading tests and corrections can be achieved. The fading corrected IRSL ages are more reliable and fit better to the stratigraphical expectations. The younger fading corrected ages (up to 50-60 ka) are consistent with the OSL ages of some quartz samples and with the radiocarbon results. The older fading corrected IRSL ages (90-130 ka) are still underestimated, very likely due to the applied correction method, which is suitable and set up for young samples, or due to the early saturation of the IRSL signal hindering the exact dating of these old samples.

Theoretically OSL dating of the quartz yields more precise ages contrary to the feldspar ages, since the quartz does not suffer from anomalous fading. Unfortunately the OSL properties of the quartz were poor in all samples. Some samples yielded results from the Tura section despite of their dim OSL signal. It is likely, that the glacial material from the Alpine region, carried by the palaeo-Danube, is responsible for the poor luminescence properties of the quartz minerals in both investigated regions.

Summarising the results, the dating of the Süttő and Tura profiles using IRSL MAAD and SAR protocols makes connection between the dating carried out in the past and will be carried out in the future. In a stratigraphical point of view the most important result, that the age of the last interglacial soil, can be found at Süttő, seems to be confirmed by chronological methods like amino acid racemization and luminescence.

Author: Qi-Shun Fan
Thesis Title: Quartz optically stimulated luminescence chronology for high lake level periods in the eastern Qaidam Basin, northeastern Qinghai–Tibetan Plateau since late Quaternary and its palaeoenvironmental implications
Grade: PhD
Date: June 2009
Supervisors: Hai-Zhou Ma and Zhong-Ping Lai
Address: Key Laboratory of Salt Lake Resources and Chemistry, Qinghai Institute of Salt Lakes, CAS, XiNing 810008, P.R.China.

Qaidam Basin is located in the northeastern Qinghai–Tibetan Plateau (QTP), which deposited many lakes (salt lakes now) and preserved a series of shorelines or highstand lacustrine sediments around some lakes. Controversy exists regarding the chronology for high lake levels of lakes in the QTP. Significant efforts have been invested to define the timing of palaeoshoreline deposits using radiocarbon dating on the QTP, and 'pan–lake period' (40~28 ka BP), 'the greatest lake period' (40~25 ka BP) or 'rather warm and humid period' (40~30 ka BP) has been proposed in Late Marine Isotope Stage (MIS) 3. Also using ^{14}C dating, similar observations were reported from adjacent regions, such as the Tengger Desert, the Badain Jaran Desert and the Taklamakan Desert in western China. In recent years, however, others argued that Qinghai Lake, located in the east

of Qaidam Basin on the northeastern QTP, developed a large lake in the period of 110–75 ka (corresponding to MIS 5). Lake level is even lower than present during MIS 3.

Therefore, the aim of this study is to establish the quartz OSL chronology, using SAR protocol, for high lake level periods in the eastern Qaidam Basin and discuss evolution history of Gahai Lake, Toson Lake and Shell Bar based on the geomorphic evidence of lakeshore sediments and environmental proxy (carbonate content) of Shell Bar section. It is concluded that:

(1) By analyzing laboratory tests (such as preheat plateau, dose recovery test, growth curves and scatter of D_e for samples), the results indicate that the SAR protocol is appropriate for D_e determination for lacustrine deposits in the eastern Qaidam Basin.

(2) OSL dating results show that high lake levels of Gahai Lake, Toson Lake and Shell Bar in the eastern Qaidam Basin occurred in MIS 5, MIS 3 and early–middle Holocene. By comparison high lake level records of lakes in study region with other lakes (Qinghai Lake, Namco Lake) on the QTP, we found that they are almost synchronous, and high lake levels are gradually dropped since MIS 5. The possible mechanism for the formation of high lake levels in the eastern Qaidam Basin was strong Asian summer monsoon.

Author: Alexander Kunz
Thesis Title: Coastal and dune evolution in south east India revealed by optically stimulated luminescence dating: Reconstruction of sediment dynamic, event history, climatic and environmental change for the last 3500 years
Grade: PhD
Date: October 2010
Supervisors: Brigitte Urban (Leuphana University Lüneburg), Manfred Frechen (Leibniz-Institute for Applied Geophysics)
Address: Faculty of Environmental Sciences and Engineering, Leuphana University, Lüneburg, Germany

Sediments in drylands or coastal areas are good archives for palaeoenvironmental studies. They preserve and reflect changes in climate, events like storms or tsunamis and human impact. The application of dating methods allows establishing a geochronological framework which can be used, e.g., to correlate periods of dune and soil formation to past dry and wet climate conditions or to estimate a recurrence interval for events like storms, tsunamis and earthquakes. The investigation of coastal areas is important as coasts are one of the most dynamic landforms and in many parts of the world densely populated. The impact of events like storms and tsunamis or climatic change has severe consequences on the ecosphere, geosphere and anthroposphere. The knowledge about coastal processes and their timing can help in developing plans for coastal protection and risk assessment.

The aim of this study was to establish a reliable chronological framework for the coastal development of the Andaman Islands and south east India. This framework was used to understand the timing of coastal processes and to reconstruct the genesis of sediments and connect them with events which are indicative for environmental and climatic changes. The dating was done using optically stimulated luminescence (OSL) and radiocarbon. Based on the physical properties of the OSL dating method it is an excellent tool to determine the depositional age of sediments.

On the Andaman Islands coastal sediments have been investigated to find evidence for palaeotsunamis and palaeoearthquakes and to reconstruct the recurrence interval for strong events like the Indian Ocean tsunami from December 2004. Sediment material from event-layers was dated using OSL and radiocarbon dating. The results show evidence for strong earthquakes at around 1000 and 3000 years before present and they reflect the storm activity for the last 1000 years. Also the complex pattern of co- and postseismic uplift and subsidence of the Andaman Islands could be reconstructed.

At the south east coast of India dunes in the Cuddalore area have been investigated. These dunes form a belt running parallel to the coast. A transect from the coast to the most western dune inland was investigated. The dunes show sedimentological features like unconformities, changes in the direction of bedding, erosional features, water escape structures and remnants of human settlement and soil-like horizons which are indicative for environmental changes. The results from the dunes show a connection between the monsoon activity for the last 3500 years and periods of sand movement and stabilisation of dunes. The younger dunes show a connection between periods of reduced rainfall and sand mobilisation for the last 200 years. The investigation of the younger dunes shows also that the dune system in the study area reacts very sensitive to changes in rainfall and disturbances in the landscape.

Based on the dating and sedimentological results of this thesis it can be concluded that the coastal areas

are very dynamic with rapidly occurring environmental changes. This research draws a clearer picture of the dynamics of coastal environments in south east India and the Andaman Islands and thus provides useful information for coastal zone management planning.

Author: Anni Madsen
Thesis Title: On the evolution of tidal basins - Absolute chronology, geomorphology and sedimentology
Grade: PhD
Date: May 2010
Supervisors: Morten Pejrup, Thorbjørn J. Andersen, Andrew S. Murray
Address: Department of Geography and Geology, University of Copenhagen, Denmark

Tidal basins and bar-built estuaries make up 13% of the world's coastlines. These areas act as important ecosystems for birds and wildlife. Low-lying sand flats within the inter-tidal zone and salt-marshes fringing these tidal basins may be severely threatened by anticipated global warming scenarios, which lead to a sealevel rise. This depends, however, to a large extent on how the sedimentation in these low-lying wetlands responds to an accelerated rate of sea-level rise.

The main objective of this study is to describe the spatial and temporal variability of sedimentation inside tidal basins in order to determine the role of sea-level variations on sedimentation in inter-tidal environments. More specifically, this study investigates whether variations in relative sea-level are the 'key driver' for sedimentation by attempting to compare inter-tidal sedimentation rates from three sites that have experienced different sea-level histories.

Sedimentation rates are determined by dating different layers in the sedimentary deposits. Absolute chronologies, obtained using luminescence dating are established from sediment cores, which were recovered in the Danish part of the Wadden Sea (Lister Dyb tidal basin) and in two estuaries in New Zealand (Whanganui Inlet and Parengarenga harbour). The luminescence dating technique assesses the period of time elapsed since quartz and/or feldspar grains were last exposed to daylight, for example as a result of sediment transport in the coastal environment. Radiocarbon dating of underlying peat deposits is used as independent age control to validate the luminescence chronology. The geomorphological and sedimentological evolution during the past few millennia is then described based on investigations of these sediment cores and associated chronologies.

Bioturbation by lugworms lead to post-depositional mixing of the surface sediments that may hamper the establishment of an absolute geochronology. The effects of bioturbation processes on the luminescence ages are therefore investigated. This is done by looking at high-resolution age-depth trends which allows the maximum age offset, the bioturbation rate and a mixing depth of ~20 cm to be determined for a sandy tidal flat in the Wadden Sea. Consequently, the upper ~20 cm of the sediment package (corresponding to 100–200 years of deposition) cannot be used to evaluate temporal trends in sedimentation rates at sandy tidal flats with lugworms, and doing this will lead to serious misinterpretations. However, sedimentary archives from inter-tidal mudflats may be useful to describe the recent (<100 years) temporal trends in sedimentation rates, because preserved sediments are more complete and less disturbed at tidal mudflats than at sandy tidal flats.

High-resolution records of the sedimentation rates of both sandy and muddy tidal deposits have been obtained, despite post-depositional mixing processes. Luminescence dating provides one of the first absolute chronologies for recent to millennial inter-tidal sand deposition in the Wadden Sea, which has been obtained with this degree of detail in time and space. The long-term sedimentation rate averaged over the last few millennia is ~0.7 mm·a-1 in Lister Dyb tidal basin. This is comparable to the relative sea-level rise, which has been observed for the last 2000 years (Szkornik et al., 2008). At a majority of the sites, the sedimentation on the tidal flats is able to keep pace with the relative sea-level rise.

The establishment of sediment budgets for sandy tidal flats is now possible, because the coarse-grained fraction of the sediment in tidal basins can be dated with luminescence dating. This offers new opportunities to the problem of determining contemporary sedimentation of sand. Budgets based on luminescence dating can provide estimates of the total sedimentation in tidal basins in contrast to previous fine-grained sediment budgets that were only based on ^{210}Pb dating.

The ratio between variations of relative sea-level and sediment supply controls the sedimentation on the tidal flats and determines whether there is a positive or negative sediment budget inside tidal basins. There is no reason to think that low-lying tidal flats are threatened in the future, as long as the sediment supply continues to be adequate. However, it is questionable whether sediment supply will be sufficient to keep up with an accelerated rate of sea-level rise as projected by all scenarios by the

Intergovernmental Panel on Climate Change (IPCC), and whether the findings from the sediment archive can be extrapolated into the future is still debatable.

Bibliography
Compiled by Daniel Richter

From 1st May 2010 to 31st October 2010

Adamiec, G., Duller, G. A. T., Roberts, H. M., and Wintle, A. G. (2010). Improving the TT-OSL SAR protocol through source trap characterisation. *Radiation Measurements* **45,** 768-777.

Ankjærgaard, C., and Jain, M. (2010). Optically stimulated phosphorescence in orthoclase feldspar over the millisecond to second time scale. *Journal of Luminescence* **130,** 2346-2355.

Ankjærgaard, C., Jain, M., Thomsen, K. J., and Murray, A. S. (2010). Optimising the separation of quartz and feldspar optically stimulated luminescence using pulsed excitation. *Radiation Measurements* **45,** 778-785.

Argyilan, E. P., Forman, S. L., and Thompson, T. A. (2010). Variability of Lake Michigan water level during the past 1000 years reconstructed through optical dating of a coastal strandplain. *The Holocene* **20,** 723-731.

Astakhov, V., and Nazarov, D. (2010). Correlation of Upper Pleistocene sediments in northern West Siberia. *Quaternary Science Reviews* **29,** 3615-3629.

Avni, Y., Zhang, J. F., Shelach, G., and Zhou, L. P. (2010). Upper Pleistocene-Holocene geomorphic changes dictating sedimentation rates and historical land use in the valley system of the Chifeng region, Inner Mongolia, northern China. *Earth Surface Processes and Landforms* **35,** 1251-1268.

Bailey, R. M. (2010). Direct measurement of the fast component of quartz optically stimulated luminescence and implications for the accuracy of optical dating. *Quaternary Geochronology* **5,** 559-568.

Balescu, S., Lamothe, M., and Panaiotu, C. (2010). IRSL chronology of eastern Romanian loess sequences. *Quaternaire* **21,** 115-126.

Baltrunas, V., Karmaza, B., Molodkov, A., Sinkunas, P., Svedas, K., and Zinkute, R. (2010). Structure, formation and geochronology of the late Pleistocene and Holocene cover deposits in South-Eastern Lithuania. *Sedimentary Geology* **231,** 85-97.

Bates, M. R., Briant, R. M., Rhodes, E. J., Schwenninger, J.-L., and Whittaker, J. E. (2010). A new chronological framework for Middle and Upper Pleistocene landscape evolution in the Sussex/Hampshire Coastal Corridor, UK. *Proceedings of the Geologists' Association* **121,** 369-392.

Benito, G., Sancho, C., Peña, J. L., Machado, M. J., and Rhodes, E. J. (2010). Large-scale karst subsidence and accelerated fluvial aggradation during MIS6 in NE Spain: climatic and paleohydrological implications. *Quaternary Science Reviews* **29,** 2694-2704.

Berger, G. W., Murray, A. S., Thomsen, K. J., and Domack, E. W. (2010). Dating ice shelf edge marine sediments: A new approach using single-grain quartz luminescence. *Journal of Geophysical Research-Earth Surface* **115**, F03003, 10.1029/2009jf001415.

Berger, G. W., Sawyer, T. L., and Unruh, J. R. (2010). Single- and Multigrain Luminescence Dating of Sediments Related to the Greenville Fault, Eastern San Francisco Bay Area, California. *Bulletin of the Seismological Society of America* **100,** 1051-1072.

Boulter, C., Bateman, M. D., and Frederick, C. D. (2010). Understanding geomorphic responses to environmental change: a 19 000-year case study from semi-arid central Texas, USA. *Journal of Quaternary Science* **25,** 889–902.

Bouquillon, A., Zink, A., and Porto, E. (2010). The Louvre Tanagras in the light of scientific analysis. Authenticity, Materials, Provenances. *In* "Tanagras -Figurines for life and eternity - The musee du louvre's collection of Greek figurines." (V. Jeammet, Ed.), pp. 286-309. Fundacion Bancaja Valencia

Cheetham, M. D., Keene, A. F., Erskine, W. D., Bush, R. T., Fitzsimmons, K., Jacobsen, G. E., and Fallon, S. J. (2010). Resolving the Holocene alluvial record in southeastern Australia using luminescence and radiocarbon techniques. *Journal of Quaternary Science* **25,** 1160-1168.

Chithambo, M. L. (2011). A time-correlated photon counting system for measurement of pulsed optically stimulated luminescence. *Journal of Luminescence* **131,** 92-98.

Chruscinska, A. (2010). On some fundamental features of optically stimulated luminescence measurements. *Radiation Measurements* **45,** 991-999.

Coelho, M. R., Martins, V. M., Vidal-Torrado, P., de Gouveia Souza, C. R., Perez, X. L. O., and Vázquez, F. M. (2010). Relationship between soil, landscape and geological substrate of the sandy coastal plain of são paulo state. *Relação solo-relevo-substrato geológico nas restingas da planície costeira do estado de são paulo* **34,** 833-846.

Cordier, S., Frechen, M., and Tsukamoto, S. (2010). Methodological aspects on luminescence dating of fluvial sands from the Moselle Basin, Luxembourg. *Geochronometria* **35,** 67-74.

de Torres, T., Ortiz, J. E., Grün, R., Eggins, S., Valladas, H., Mercier, N., Tisnérat-Laborde, N., Juliá, R., Soler, V., Martínez, E., Sánchez-Moral, S., Canaveras, J. C., Lario, J., Badal, E., Lalueza-Fox, C., Rosas, A., Santamría, D., de la Rasilla, M., and Fortea, J. (2010). Dating of the Hominoid (Homo Neanderthalensis) remains accumulation from el Sidrón cave (Piloña, Asturias, North Spain): An example of a multi-methodological approach to the dating of upper pleistocene sites. *Archaeometry* **52,** 680-705.

Deeben, J., Hiddink, H., Huisman, D. J., Müller, A., Schokker, J., and Wallinga, J. (2010). Middle Palaeolithic artefact migration due to periglacial processes; a geological investigation into near-surface occurrence of Palaeolithic artefacts (Limburg-Eastern Brabant coversand region, the Netherlands). *Geologie en Mijnbouw/Netherlands Journal of Geosciences* **89,** 35-50.

Dehnert, A., Preusser, F., Kramers, J. D., AkÇAr, N., Kubik, P. W., Reber, R., and SchlÜChter, C. (2010). A multi-dating approach applied to proglacial sediments attributed to the most extensive glaciation of the Swiss Alps. *Boreas* **39,** 620-632.

Dreibrodt, S., Lomax, J., Nelle, O., Lubos, C., Fischer, P., Mitusov, A., Reiss, S., Radtke, U., Nadeau, M., Grootes, P. M., and Bork, H.-R. (2010). Are mid-latitude slopes sensitive to climatic oscillations? Implications from an Early Holocene sequence of slope deposits and buried soils from eastern Germany. *Geomorphology* **122,** 351-369.

Enzel, Y., Amit, R., Crouvi, O., and Porat, N. (2010). Abrasion-derived sediments under intensified winds at the latest Pleistocene leading edge of the advancing Sinai-Negev erg. *Quaternary Research* **74,** 121-131.

Fattibene, P., and Callens, F. (2010). EPR dosimetry with tooth enamel: A review. *Applied Radiation and Isotopes* **68,** 2033-2116.

Feathers, J., Kipnis, R., Piló, L., Arroyo-Kalin, M., and Coblentz, D. (2010). How old is Luzia? Luminescence dating and stratigraphic integrity at Lapa Vermelha, Lagoa Santa, Brazil. *Geoarchaeology* **25,** 395-436.

Fedorowicz, S., and Gaigalas, A. (2010). Geochronological and Sedimentological Interpretation of Interglacial Aquatic Sediments based on TL Dating. *Geochronometria* **35,** 75-83.

Ferreira de Souza, L. B., Guzzo, P. L., and Khoury, H. J. (2010). Correlating the TL response of γ-irradiated natural quartz to aluminum and hydroxyl point defects. *Journal of Luminescence* **130,** 1551-1556.

Fitzsimmons, K. E., and Barrows, T. T. (2010). Holocene hydrologic variability in temperate southeastern Australia: An example from Lake George, New South Wales. *The Holocene* **20,** 585-597.

Gabor, A. T., Vasiliniuc, Ş., Bădărău, A. S., Begy, R., and Cosma, C. (2010). Testing the potential of optically stimulated luminescence dating methods for dating soil covers from the forest steppe zone in Transylvanian Basin. *Carpathian Journal of Earth and Environmental Sciences* **5,** 137-144.

Ganzawa, Y. (2010). Red thermoluminescence (RTL) sensitivity change in quartz. *Radiation Measurements* **45,** 985-990.

Garcia-Guinea, J., Correcher, V., Rodriguez-Lazcano, Y., Crespo-Feo, E., and Prado-Herrero, P. (2010). Light emission bands in the radioluminescence and thermoluminescence spectra of kaolinite. *Applied Clay Science* **49,** 306-310.

Grapes, R. H., Rieser, U., and Wang, N. (2010). Reply to Lowe, D.J., Wilson, C.J.N., Newnham, R.M., Hogg, A.G. comment on Grapes, R., Rieser, U., Wang, N., 2010. Optical luminescence dating of a loess section containing a critical tephra marker horizon, SW North Island of New Zealand. *Quaternary Geochronology* **5,** 497-501.

Gueli, A. M., Stella, G., Troja, S. O., Burrafato, G., Fontana, D., Ristuccia, G. M., and Zuccarello, A. R. (2010). Historical buildings: Luminescence dating of fine grains from bricks and mortar. *Nuovo Cimento della Societa Italiana di Fisica B* **125,** 719-729.

Halfen, A. F., Fredlund, G. G., and Mahan, S. A. (2010). Holocene stratigraphy and chronology of the Casper Dune Field, Casper, Wyoming, USA. *The Holocene* **20,** 773-783.

Hall, S. A., Miller, M. R., and Goble, R. J. (2010). Geochronology of the Bolson sand sheet, New Mexico and Texas, and its archaeological significance. *Geological Society of America Bulletin* **122,** 1950-1967.

Harvey, J. A., Haverland, N. P., and Kearfott, K. J. (2010). Characterization of the glow-peak fading properties of six common thermoluminescent materials. *Applied Radiation and Isotopes* **68,** 1988-2000.

Haws, J. A., Benedetti, M. M., Funk, C. L., Bicho, N. F., Daniels, J. M., Hesp, P. A., Minckley, T. A., Forman, S. L., Jeraj, M., Gibaja, J. F., and Hockett, B. S. (2010). Coastal wetlands and the Neanderthal settlement of Portuguese Estremadura. *Geoarchaeology* **25,** 709-744.

Helmens, K. F., and Engels, S. (2010). Ice-free conditions in eastern Fennoscandia during early Marine Isotope Stage 3: Lacustrine records. *Boreas* **39,** 399-409.

Herman, F., Rhodes, E. J., Braun, J., and Heiniger, L. (2010). Uniform erosion rates and relief amplitude during glacial cycles in the Southern Alps of New Zealand, as revealed from OSL-thermochronology. *Earth And Planetary Science Letters* **297,** 183-189.

Hollingsworth, J., Fattahi, M., Walker, R., Talebian, M., Bahroudi, A., Bolourchi, M. J., Jackson, J., and Copley, A. (2010). Oroclinal bending, distributed thrust and strike-slip faulting, and the accommodation of Arabia-Eurasia convergence in NE Iran since the Oligocene. *Geophysical Journal International* **181,** 1214-1246.

Holt, K. A., Wallace, R. C., Neall, V. E., Kohn, B. P., and Lowe, D. J. (2010). Quaternary tephra marker beds and their potential for palaeoenvironmental reconstruction on Chatham Island, east of New Zealand, southwest Pacific Ocean. *Journal of Quaternary Science* **25,** 1169–1178.

Jacobs, Z. (2010). An OSL chronology for the sedimentary deposits from Pinnacle Point Cave 13B--A punctuated presence. *Journal of Human Evolution* **59,** 289-305.

Jaek, J., Molod'kov, A., and Vasil'chenko, V. (2010). Mechanisms of luminescent responses in thermal and optical stimulation of potassium feldspars. *Journal of Applied Spectroscopy* **77,** 441-444.

Kadereit, A., Kühn, P., and Wagner, G. A. (2010). Holocene relief and soil changes in loess-covered areas of south-western Germany: The pedosedimentary archives of Bretten-Bauerbach (Kraichgau). *Quaternary International* **222,** 96-119.

Kiyak, N. G., and Erginal, A. E. (2010). Optical stimulated luminescence dating study of eolianite on the Island of Bozcaada, Turkey: Preliminary results. *Journal of Coastal Research* **26,** 673-680.

Kunz, A., Frechen, M., Ramesh, R., and Urban, B. (2010). Luminescence dating of late holocene dunes showing remnants of early settlement in Cuddalore and evidence of monsoon activity in south east India. *Quaternary International* **222,** 194-208.

Küster, M., and Preusser, F. (2009). Late Glacial and Holocene aeolian sands and soil formation from the Pomeranian outwash plain (Mecklenburg, NE-Germany). *Eiszeitalter und Gegenwart / Quarternary Science Journal* **58,** 156–163.

Lauer, T., Frechen, M., Hoselmann, C., and Tsukamoto, S. (2010). Fluvial aggradation phases in the Upper Rhine Graben--new insights by quartz OSL dating. *Proceedings of the Geologists' Association* **121,** 154-161.

Liberda, J. J., Thompson, J. W., Rink, W. J., Quirós, F. B. d., Jayaraman, R., Selvaretinam, K., Chancellor-Maddison, K., and Volterra, V. (2010). ESR dating of tooth enamel in Mousterian layer 20, El Castillo, Spain. *Geoarchaeology* **25,** 467-474.

Liritzis, I., Drivaliari, N., Polymeris, G. S., and Katagas, C. (2010). New quartz technique for OSL dating of limestones. *Mediterranean Archaeology and Archaeometry* **10,** 81-87.

Long, H., Lai, Z., Wang, N., and Li, Y. (2010). Holocene climate variations from Zhuyeze terminal lake records in East Asian monsoon margin in arid northern China. *Quaternary Research* **74,** 46-56.

Loope, H. M., Loope, W. L., Goble, R. J., Fisher, T. G., Jol, H. M., and Seong, J. C. (2010). Early Holocene dune activity linked with final destruction of Glacial Lake Minong, eastern Upper Michigan, USA. *Quaternary Research* **74,** 73-81.

Lowe, D. J., Wilson, C. J. N., Newnham, R. M., and Hogg, A. G. (2010). Dating the Kawakawa/Oruanui eruption: Comment on "Optical luminescence dating of a loess section containing a critical tephra marker horizon, SW North Island of New Zealand" by R. Grapes et al. *Quaternary Geochronology* **5,** 493-496.

Lowick, S. E., Preusser, F., Pini, R., and Ravazzi, C. (2010). Underestimation of fine grain quartz OSL dating towards the Eemian: Comparison with palynostratigraphy from Azzano Decimo, northeastern Italy. *Quaternary Geochronology* **5,** 583-590.

Lowick, S. E., Preusser, F., and Wintle, A. G. (2010). Investigating quartz optically stimulated luminescence dose-response curves at high doses. *Radiation Measurements* **45,** 975-984.

Lüthgens, C., Böse, M., and Krbetschek, M. (2010). On the age of the young morainic morphology in the area ascribed to the maximum extent of the Weichselian glaciation in north-eastern Germany. *Quaternary International* **222,** 72-79.

Madsen, A. T., Murray, A. S., Andersen, T. J., and Pejrup, M. (2010). Spatial and temporal variability of sediment accumulation rates on two tidal flats in Lister Dyb tidal basin, Wadden Sea, Denmark. *Earth Surface Processes and Landforms* **35,** 1556–1572.

Mandowski, A., Orzechowski, J., and Mandowska, E. (2010). Kinetics of excitation in TL and OSL detectors. *Optical Materials* **32,** 1568-1572.

Manfred, M. E., Gabriel, N. T., Yukihara, E. G., and Talghader, J. J. (2010). Thermoluminescence measurement technique using millisecond temperature pulses. *Radiation Protection Dosimetry* **139,** 560-564.

Martins, A. A., Cunha, P. P., Rosina, P., Osterbeek, L., Cura, S., Grimaldi, S., Gomes, J., Buylaert, J.-P., Murray, A. S., and Matos, J. (2010). Geoarchaeology of Pleistocene open-air sites in the Vila Nova da Barquinha-Santa Cita area (Lower Tejo River basin, central Portugal). *Proceedings of the Geologists' Association* **121,** 128-140.

Niedermayer, M., and Bayer, A. (2010). Pulsed Photon-Stimulated Luminescence (PPSL) as a tool in retrospective dosimetry. *Radiation Protection Dosimetry* **139,** 494-504.

Nielsen, A. H., Elberling, B., and Pejrup, M. (2010). Soil development rates from an optically stimulated luminescence-dated beach ridge sequence in Northern Jutland, Denmark. *Canadian Journal of Soil Science* **90,** 295-307.

Novothny, Á., Frechen, M., and Horváth, E. (2010). Luminescence dating of periods of sand movement from the Gödöllo Hills, Hungary. *Geomorphology* **122,** 254-263.

Outram, Z., Batt, C. M., Rhodes, E. J., and Dockrill, S. J. (2010). The integration of chronological and archaeological information to date building construction: an example from Shetland, Scotland, UK. *Journal of Archaeological Science* **37,** 2821-2830.

Pawley, S. M., Toms, P., Armitage, S. J., and Rose, J. (2010). Quartz luminescence dating of Anglian Stage (MIS 12) fluvial sediments: Comparison of SAR age estimates to the terrace chronology of the Middle Thames valley, UK. *Quaternary Geochronology* **5,** 569-582.

Ray, Y., and Srivastava, P. (2010). Widespread aggradation in the mountainous catchment of the Alaknanda-Ganga River System: timescales and implications to Hinterland-foreland relationships. *Quaternary Science Reviews* **29,** 2238-2260.

Rehak, K., Niedermann, S., Preusser, F., Strecker, M. R., and Echtler, H. P. (2010). Late Pleistocene landscape evolution in south-central Chile constrained by luminescence and stable cosmogenic nuclide dating. *Bulletin of the Geological Society of America* **122,** 1235-1247.

Reimann, T., Naumann, M., Tsukamoto, S., and Frechen, M. (2010). Luminescence dating of coastal sediments from the Baltic Sea coastal barrier-spit Darss-Zingst, NE Germany. *Geomorphology* **122,** 264-273.

Richter, D. (2010). Thermoluminescence dating of heated flint artefacts from Ifri n'Ammar. *In* "La Grotte d'Ifri n'Ammar. Le Paléolithique Moyen." (M. Nami, and J. Moser, Eds.), pp. 325-337. Forschungen zur Archäologie Außereuropäischer Kulturen. Reichert Verlag, Wiesbaden.

Richter, D., Dombrowski, H., Neumaier, S., Guibert, P., and Zink, A. C. (2010). Environmental gamma dosimetry with OSL of α-Al_2O_3:C for in situ sediment measurements. *Radiation Protection Dosimetry* **141,** 27-35.

Richter, D., Moser, J., Nami, M., Eiwanger, J., and Mikdad, A. (2010). New chronometric data from Ifri n'Ammar (Morocco) and the chronostratigraphy of the Middle Palaeolithic in the Western Maghreb. *Journal of Human Evolution* **59,** 672-679.

Rink, W. J., and López, G. I. (2010). OSL-based lateral progradation and aeolian sediment accumulation rates for the Apalachicola Barrier Island Complex, North Gulf of Mexico, Florida. *Geomorphology* **123,** 330-342.

Sarala, P., Pihlaja, J., Putkinen, N., and Murray, A. (2010). Composition and origin of the middle Weichselian interstadial deposit in Veskoniemi, Northern Finland. *Estonian Journal of Earth Sciences* **59,** 117-124.

Shulmeister, J., Thackray, G. D., Rieser, U., Hyatt, O. M., Rother, H., Smart, C. C., and Evans, D. J. A. (2010). The stratigraphy, timing and climatic implications of glaciolacustrine deposits in the middle Rakaia Valley, South Island, New Zealand. *Quaternary Science Reviews* **29,** 2362-2381.

Sierralta, M., Kele, S., Melcher, F., Hambach, U., Reinders, J., van Geldern, R., and Frechen, M. (2010). Uranium-series dating of travertine from Sütto: Implications for reconstruction of environmental change in Hungary. *Quaternary International* **222,** 178-193.

Sinha, S., Suresh, N., Kumar, R., Dutta, S., and Arora, B. R. (2010). Sedimentologic and geomorphic studies on the Quaternary alluvial fan and terrace deposits along the Ganga exit. *Quaternary International* **227,** 87-103.

Stauch, G., and Lehmkuhl, F. (2010). Quaternary glaciations in the Verkhoyansk Mountains, Northeast Siberia. *Quaternary Research* **74,** 145-155.

Stevens, T., and Lu, H. (2010). Radiometric dating of the late Quaternary summer monsoon on the Loess Plateau, China, pp. 87-108. Geological Society Special Publication 342.

Thakur, V. C., Pandey, A. K., Nautiyal, C. M., Sundriyal, Y. P., Khanduri, B. M., Shinde, D. P., Suresh, N., and Singhvi, A. K. (2010). Geo-Archeology at Khajnawar in Western Uttar Pradesh plain. *Current Science* **98,** 1112-1119.

Thamó-Bozsó, E., Magyari, Á., Musitz, B., and Nagy, A. (2010). OSL ages and origin of Late Quaternary sediments in the North Transdanubian Hills (Hungary): timing of neotectonic activity. *Quaternary International* **222,** 209-220.

Thiel, C., Coltorti, M., Tsukamoto, S., and Frechen, M. (2010). Geochronology for some key sites along the coast of Sardinia (Italy). *Quaternary International* **222,** 36-47.

Wallinga, J., and Bos, I. J. (2010). Optical dating of fluvio-deltaic clastic lake-fill sediments - A feasibility study in the Holocene Rhine delta (western Netherlands). *Quaternary Geochronology* **5,** 602-610.

Westaway, K. E., Sutikna, T., Morwood, M. J., and Zhao, J.-X. (2010). Establishing rates of karst landscape evolution in the Tropics: a context for the formation of archaeological sites in western Flores, Indonesia. *Journal of Quaternary Science* **25,** 1018–1037.

Xu, L., Ou, X., Lai, Z., Zhou, S., Wang, J., and Fu, Y. (2010). Timing and style of Late Pleistocene glaciation in the Queer Shan, northern Hengduan Mountains in the eastern Tibetan Plateau. *Journal of Quaternary Science* **25,** 957–966.

Yang, L., Zhou, J., Lai, Z., Long, H., and Zhang, J. (2010). Lateglacial and Holocene dune evolution in the Horqin dunefield of northeastern China based on luminescence dating. *Palaeogeography, Palaeoclimatology, Palaeoecology* **296,** 44-51.

Yanites, B. J., Tucker, G. E., Mueller, K. J., Chen, Y. G., Wilcox, T., Huang, S. Y., and Shi, K. W. (2010). Incision and channel morphology across active structures along the Peikang River, central Taiwan: Implications for the importance of channel width. *Bulletin of the Geological Society of America* **122,** 1192-1208.

Zhang, J.-F., Huang, W.-W., Yuan, B.-Y., Fu, R.-Y., and Zhou, L.-P. (2010). Optically stimulated luminescence dating of cave deposits at the Xiaogushan prehistoric site, northeastern China. *Journal of Human Evolution* **59,** 514-524.

Zink, A. (2009). Luminescence date and archaeological ages: An epistemology of the luminescence dating. *In* "Proceedings of the XV World Congress UISPP/ Actes du XV Congrès Mondial (Lisbon, 4-9 September 2006), vol. 32." (L. Oosterbeek, Ed.), pp. 113-116. British Archaeological Reports, International Series 2045. Archaeopress.

Zink, A. J. C., Dabis, S., Porto, E., and Castaing, J. (2010). Alpha efficiency under TL and OSL - A subtraction technique using OSL and TL to detect artificial irradiation. *Radiation Measurements* **45,** 649-652.

Conference Announcements

13th International Conference on Luminescence and Electron Spin Resonance Dating (LED 2011)

10^{th}-14^{th} July 2011

The conference will take place at the Faculty of Mathematics and Computer Science of the Nicolaus Copernicus University in Toruń, Poland between 10th and 14th July 2011. It is planned for the conference to commence on Sunday morning (10th). The Rectors of both Universities took an honorary patronage over the Conference.

The conference is addressed to researchers developing dating methods relying on trapped charge methods (luminescence and electron spin resonance) and to applying those methods in a wide variety of absolute dating problems. The topics include heated and unheated Quaternary geological, geo-morphological and archaeological materials, fundamental studies of basic physical phenomena and related dosimetry as well as advances in instrumentation.

The city of Toruń, founded in 1231, is a treasure of Polish and European history, most importantly, famous for being the home to Nicolaus Copernicus. The city is famous for its remarkable monuments which have won the designation of the cultural heritage of mankind from UNESCO and is visited by a large number of tourists each year.

The conference will be followed up by an optional 4-day (15th to 18th July 2011) post-conference trip to several places of interest in north and south Poland (Medieval castle of Malbork, site of Wapienno and Biskupin, caves near Kraków in the so-called Polish Jurassic Highland, Wieliczka salt mine – UNESCO World Heritage site and the city of Kraków). The trip will conclude in Kraków on 18th July, 2011.

Important deadlines:

28 February 2011: Registration and submission of abstracts

31 March 2011: Early payment

Further information about the meeting can be found at http://led2011.polsl.pl

On behalf of the organising Committee of LED 2011

PRIFYSGOL ABERYSTWYTH UNIVERSITY

UK Luminescence and ESR meeting

12th-14th September 2012

The next UK luminescence and ESR dating research meeting will be held at Aberystwyth University from the 12-14th September 2012. The meeting is intended to provide a forum for the presentation and discussion of the latest research in luminescence and ESR dating and related work. Presentations covering basic physics, methodological issues and the application of these techniques are all welcome. The meeting will consist of both oral and poster presentations, and presentations by research students are particularly encouraged.

Further details will be posted on the Aberystwyth Luminescence Research Laboratory website (http://www.aber.ac.uk/en/iges/research-groups/quaternary/luminescence-research-laboratory) later in 2011.

Professor Geoff Duller
Dr Helen Roberts

Institute of Geography and Earth Sciences,
Aberystwyth University,
Ceredigion, SY23 3DB,
United Kingdom

Errata: An alternate form of probability-distribution plots for D_e values

G. W. Berger

Desert Research Institute, 2215 Raggio Parkway, Reno, NV 89512, USA
(e-mail: glenn.berger@dri.edu)

(Received 5 December 2010)

Errata

In the paper by Berger (2010), there are two errors. In the first the author stated that radial plots are not applicable to D_e distributions containing negative D_e values. This is correct only if a logarithmic scale is used (as in the widely circulated radial-plot graphical routine by Olley). The author's statement is incorrect if a linear scale for D_e values is used (e.g., Fig. 1 in Berger, 2010, from Galbraith, 1988, and of course in Galbraith, 2010, Fig. 3).

The second error is that the author referred to the transformed PD plot as a 'relative probability' plot. This is incorrect because a $(D_e)^{-1}$ factor [in the partial-derivative transformation of $\log_e (D_e)$] was omitted. The $(D_e)^{-1}$ factor was omitted to create a plot yielding roughly constant peak heights for the example data in Fig. 3 of Berger (2010). As such the so-called TPD plot does not manifest relative probabilities (requiring comparison of areas under these peaks), rather something more akin to relative 'weighted' frequencies. If the $(D_e)^{-1}$ term is retained, then the TPD solid curve in the Fig. 3 of Berger (2010) would look closely alike the original dashed curve in that Fig. 3 (obtained using weighting by absolute errors). Thus the TPD plot (when presented with ranked D_e values) serves as only a visualization of relative (within the range of D_e values) 'weighted' frequencies when errors in D_e are mainly constant relative and when the distribution of D_e values is approximately log-normal. Finally, D_e values in the TPD plot were placed on a linear scale because generally we perceive geological time as linear, not logarithmic.

As Berger (2010) and Galbraith (2010) both agree, the appropriate post-visualization steps for calculating usefully accurate and precise age estimates involve the suitable use of either weighted means, minimum-age-models (MAM), central-age-models, etc., coupled sometimes with the display of data in a radial plot.

Acknowledgements

I thank Rex Galbraith for pointing out (pers. comm., 2010) that the omission of the $(D_e)^{-1}$ factor precludes inferring relative probabilities from the TPD plot.

References

Berger, G.W. (2010) An alternate form of probability-distribution plots for D_e values. *Ancient TL* **28**, 11-21.

Galbraith, R.F. (1988) Graphical display of estimates having differing standard errors. *Technometrics* **30**, 271-281.

Galbraith, R.F. (2010) On plotting OSL equivalent doses. *Ancient TL* **28**, 1-9.

Submission of articles to Ancient TL

Reviewing System

In order to ensure acceptable standards and minimize delay in publication, a modification of the conventional refereeing system has been devised for Ancient TL:

Articles can be sent directly by authors to a member of the Reviewers Panel chosen on the basis of the subject matter, but who is not in any of the authors' laboratories. **At the discretion of the Editor**, reviewers who are not listed in the Panel may be used.

The reviewing system aims to encourage direct dialogue between author and reviewer. The Editor should be kept advised of the progress of articles under review by sending him copies of all correspondence. He is available for advice where reviewing difficulties have arisen. Authors whose mother tongue is not English are required to have their manuscript revised for English *before* submitting it.

We ask reviewers to specify (where required) the minimum of revision that is consistent with achieving a clear explanation of the subject of the paper, the emphasis being on *rapid* publication; reviewers are encouraged to make a brief written comment for publication at the end of the paper. Where a contribution is judged not to meet an adequate standard without substantial modification, the author will be advised that the contribution is not suitable for publication. Articles that are not considered to be of sufficient interest may also be rejected.

Procedures

1. Articles should be submitted to an appropriate member of the Reviewing Panel or Editorial Board, chosen on the basis of the subject matter, but who is not in any of the authors' laboratories.
2. Articles should not normally exceed the equivalent of 5000 words inclusive of diagrams, tables and references. Greater space will be appropriate for certain topics; for these the Editor should first be consulted. Short notes and letters are also acceptable. Text should be double-spaced.
3. Diagrams and labels should be ready for direct reproduction (i.e. 1:1 camera ready) and not normally exceed 12 cm wide by 10 cm high. Where possible, high quality electronic versions of figures should also be submitted. Separate figure captions should be supplied. By ensuring that these requirements are met, authors will be able to examine whether **all** details of their diagrams are clear to the reader. Inappropriately scaled drawings and labels will be returned for alteration.
4. Authors are asked to submit 1 copy of the paper, including diagrams, to the Reviewer and a duplicate copy to the Editor.

   In addition to a hard copy of the accepted version of the paper and original diagrams, the final version of the text must be submitted to the Editor electronically using a standard format (Microsoft Word for PC is currently used for producing Ancient TL). Electronic copies of Diagrams and Tables should also be submitted.
5. Upon receipt of an article, the Editor will send an acknowledgement to the author. If the Reviewer is unable to deal with the contribution within **4 weeks** he/she will inform the author and advise the Editor.

Requirements under various situations

When agreement concerning an article has been reached:
The Editor should receive a copy of the final version of the paper, both as hard copy and electronically. The Reviewer should send their final decision, including comments for publication if any, to the Editor.

If the article has not been rejected, but agreement on its final form cannot be reached or where there are protracted delays in the reviewing process:
The Editor may request an assessment from the Reviewer and responsibility passes to the Editor.

If the article is rejected:
The Editor and author receive notification from the Reviewer, with an indication of the reason for rejection.

Thesis abstracts are to be sent to the Editor and in principle do not need reviewing. However, authors are requested to make sure that the English is correct before submission. Thesis abstracts should not exceed 500 words, and figures and tables are not accepted.

Advertising. Formal information on equipment can be published in Ancient TL. It should not exceed one printed page. Current charges are displayed on the website (http://www.aber.ac.uk/ancient-tl)

Subscriptions to Ancient TL

Ancient TL is published 2 times a year and is sent Airmail to subscribers outside the United Kingdom. While every attempt will be made to keep to publication schedule, the Editorial Board may need to alter the number and frequency of issues, depending on the number of available articles which have been accepted by reviewers.

The subscription rate for 2011 is £15 for individual subscribers and £25 for Institutional subscription, plus any taxes where required. Payment must be in pounds sterling. Enquiries and orders must be sent to the Editor. Payment may be by cheques, made payable to 'Aberystwyth University', by credit/debit cards or by bank transfers. Further information on subscriptions is available on the Ancient TL web site (**http://www.aber.ac.uk/ancient-tl**)